JOTCS B
Journal of the Turkish Chemical Society
Section: B
Chemical Engineering
TURKISH CHEMICAL SOCIETY

Classification of Zinc-Coated Parts in Accordance with their Brightness Degree using Deep Learning Techniques

Ramazan Katırcı[1*], Hasan Metehan Akgün[2], Bilal Tekin[3], Osman Gökhan Kömürkaya[3], Metin Zontul[4], and Oğuz Kaynar[5].

[1] Metallurgical and Materials Engineering, Sivas University of Science and Technology, Sivas, Turkey
[2] Aircraft Technology, Sivas University of Science and Technology, Sivas, Turkey
[3] Computer Engineering, Sivas University of Science and Technology, Sivas, Turkey
[4] Computer Engineering, Istanbul Ayvansaray University, Istanbul, Turkey
[5] Management Information Systems, Sivas Cumhuriyet University, Sivas, Turkey

Abstract: A novel technique was suggested to measure the brightness of the coated parts. The algorithm of Mask RCNN was used to detect the relevant region on the whole image. The pixels of black lines, which are associated with the brightness of the coating and reflected from the foreground, were counted using image processing technique. These pixels were used as the output in the machine learning training to classify the coated parts. The output was binarized to classify the coated plates as “Pass” and “Fail”. It was found that the RF model was the best model. The scores of its accuracy, F1, precision, and recall were established to be 0.97, 0.97, 1, and 0.94, respectively. The overlap scores of Mask RCNN were found to be in the range of 0.92-0.97, which proved that Mask RCNN algorithm detected the concerned region with high precision and accuracy.

Keywords: Mask RCNN, Deep learning, Machine learning, Zinc electroplating, Brightness measurement, Image processing, Surface detection.

Submitted: August 05, 2022. **Accepted:** October 13, 2022.

Cite this: Katırcı R, Akgün HM, Tekin B, Kömürkaya OG, Zontul M, Kaynar O. Classification of Zinc-Coated Parts in Accordance with their Brightness Degree using Deep Learning Techniques. JOTCSB. 2022;5(2):145–56.

***Corresponding author. E-mail:** ramazankatirci@sivas.edu.tr.

INTRODUCTION

Engineering components are widely fabricated to meet the expectations in the industrial applications in the world. While these components are produced, some technical requirements such as corrosion, safety, and service lifetime should be considered (1). The surface treatment methods are one of the most important techniques used to enhance the performance and properties of the materials (2). Coating, chemical treatment, painting and anodic oxidation are some of the techniques used widely in the world (3). Coating techniques can be classified as two groups; dry technique and wet technique. As an example to dry technique, thermal spraying, and sputtering methods can be given (4,5). As for the wet technique, electroplating and sol-gel method can be presented (6,7). The electroplating method has many advantages such as running in atmospheric conditions, and not requiring high pressure and temperature (8). The electroplating parameters such as additives, pH, temperature and current density, influence the coating properties and performance. Especially, organic additives added to the electroplating bath enhance the appearance, throwing power, and covering power of the coating (9). Electroplating is applied for two purposes, decorative and industrial application. While in decorative purpose, the brightness, of the coating (its appearance) is significant, in industrial purpose, hardness, corrosion, and wear resistance are crucial. In order to acquire bright coating, some special organic additives are added to the zinc, copper, nickel, and chromium electroplating bath. These organic additives decrease the crystal size and provide the brightness to the coating (10). Zinc electroplating is commonly implemented for corrosion protection (11).

Zinc electroplating processes are generally applied with three different techniques. These techniques are called acidic, alkaline, and cyanide zinc electroplating processes. Zinc coating acquired from the acidic zinc electroplating bath is very significant because it provides very bright and

flexible coating (12). To measure the brightness of the coating, a glossmeter instrument is generally used. To acquire the brightness of the entire coated surface using glossmeter, many measurements should be taken. It is however very easy to distinguish between a bright and matte surface by human eye. We think that the artificial intelligence methods are promising methods to measure the brightness of the coating using camera-based system. Katırcı et al. used the artificial intelligence method to classify the chromium coating in accordance with the appearance of the coating (8). Also, Wang et al. implemented the artificial intelligent method to identify the particle size and shape of granular materials (13).

Many artificial methods are used in engineering applications (14-17). These methods can be divided into two categories, machine learning and deep learning. In recent years, deep learning techniques have been developing at a dizzying speed. Convolutional neural network (CNN) methods such as VGG (18), ResNet (19), Inception (20) and Xception (21) are the most popular methods. Mask RCNN is a technique used for object segmentation. It uses the backbone of ResNet 101. This method detects objects and generates high-quality segmentation mask for each instance (22).

In the industry, many objects next to the coated part may have an interference effect to detect the concerned object. Therefore, Mask RCNN method can be used to extract the irrelevant data from the sample (8). The image processing technique is used to extract the features from the image data. Various image processing techniques such as thresholding and binarization can be used for this purpose (23).

In our study, to simulate the electroplating bath in the industrial conditions, Hull-cell method developed by R.O.Hull in 1939 was used (24). Hull-cell panels were coated in the acidic zinc electroplating baths prepared using the different composition. Mask RCNN and image processing techniques were used together to extract the relevant data from the images taken from the Hull-cell panels. Machine learning and deep learning technique, including gaussian process (GP), random forest (RF), support vector classifier (SVR), XGBoost (XGB), multilayer perceptron (MLP) were used to classify the appearance (brightness) of coated part in accordance with the zinc electroplating bath. Image processing techniques were used to determine the degree of brightness of the coating by counting the pixels on the black lines.

MATERIALS AND METHODS

The acidic zinc electroplating was carried out using a Thurlby 30V1A-model DC model direct-current generator. The organic additives were added to the acidic zinc electroplating bath at the values in Table 1. The 74 experiments were designed in different concentrations of the additives. The basic zinc electroplating bath consists of 80 g/L $ZnCl_2$ and 200 g/L NH_4Cl compounds in water. The overall experimental design was presented in Table S1 (in supplementary material).

Table 1. The additive ranges used in the acidic zinc electroplating bath.

		LEVELS						
Abbreviations	**Chemical names**	**1**	**2**	**3**	**4**	**5**	**6**	**7**
PA (mL/L)	Propargyl alcohol	5	10	20				
NP10 (mL/L)	Nonylphenol ethoxylate	0.25	1	2	2.75	5.25	10	10.25
BA (g/L)	Benzal acetone	0.2	0.5	1	5			
NA (g/L)	Nicotinic acid	0.2	0.5	1				
SB (g/L)	Sodium benzoate	1	2	4				
EHS (mL/L)	Ethylhexyl sulfate	10	15	25	30	40		
OCB (mL/L)	2-Chlorobenzaldehyde	2	3	5				
TAMOL (g/L)	Naphthalene sulfonate formaldehyde condensate, sodium salt	1	5	10				

The Hull-cell equipment where the panels were coated using the bath compositions in Table S1 is presented in Figure 1.

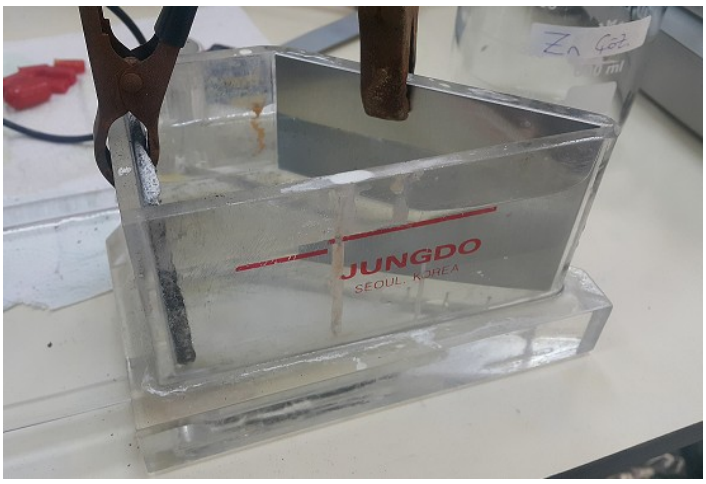

Figure 1: Hull-cell set-up used in the zinc electroplating.

Mask RCNN algorithm, which uses the backbone of ResNet 101, was used to extract the relevant data from the images. It composes of three steps; 1) extracting the feature map from the input images, 2) sending it to the Region Proposal Network (RPN) for creating region recommendations from the feature maps, 3) transferring the proposed regions to the fully connected layer for target localization, and obtaining the expected outputs. The architecture of Mask RCNN is presented in Figure 2. Mask RCNN algorithm was downloaded from the github repository: https://github.com/matterport/Mask_RCNN and the codes were adapted to our study. All networks were trained in 50 epochs.

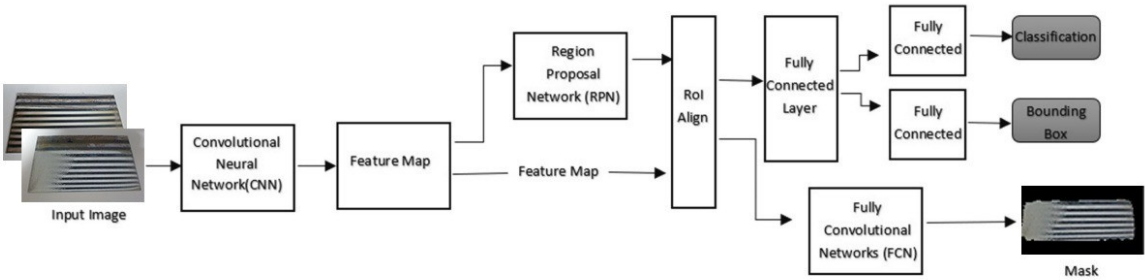

Figure 2: The architecture of Mask RCNN.

Machine learning algorithms and deep learning technique were performed to classify the quality of the plates depending on their surface brightness. The surface brightness was acquired counting the pixels between 0 and 75 on the black lines in grayscale image (0-255). The image processing technique was used to count the pixels. The pixel count was performed on the extracted data from the image. The number of pixels on the black lines reflected from the foreground were defined as the output for zinc electroplating bath. To classify the quality of the plates according to their brightness, the threshold was specified. The plates above this threshold were coded as 1 (Pass). Those below this threshold were coded as 0 (Fail). OpenCV library was used to count the black pixels. All codings were carried out using python language. Gaussian process (GP), random forest (RF), support vector classifier (SVC), XGBoost (XGB) and multilayer perceptron (MLP) algorithms were used to train the bath composition against the brightness of the coating. The hyperparameters of the models were optimized using gridsearch method. The outputs are presented under the folder of "HyperparameterOpt" in the supplementary material.

Gaussian Process (GP)

GP is a supervised learning that can be used for regression and classification based on the Gaussian probability distribution. Gaussian probability distribution functions show the distribution of random variables. GP calculates the probability of the outcome of the input data. And it works well with small datasets, high accuracy rate is achieved (25).

Random Forest (RF)

RF is a supervised learning method consisting of decision trees designed by Breiman. The decision trees were generated by selecting random samples from the train dataset. When making a prediction with these trees, the predictions of all trees are used. The decision is taken by majority vote. The prediction taking the most votes is selected. RF is used for regression and classification. It has wide usage areas such as ecology, genetics, bioinformatics and medicine (26).

Support Vector Classifier (SVC)
SVM is a supervised learning method used for classification, regression, and outlier detection. SVM tries to find the optimal hyperplane that divides the data into two parts. This hyperplane keeps the distance between the two parts at the maximum level. It maximizes the distance between the nearest points in different segments. If the data is not linear and is not divided into two parts, it can be used in nonlinear data by increasing the plane size with the help of kernel functions (27).

XGBoost (XGB)
XGBoost is an optimized supervised machine learning algorithm based on the Gradient Boosting algorithm. It became popular with the article written by Tianqi Chen and Carlos Guestrin and its usage has increased. Since it is based on the Gradient Boosting algorithm, it creates weak learning models and combines them into advanced models. With the help of the aim function, it prevents overfitting and increases performance. XGBoost is an ensemble learning based algorithm like RF, but newer than RF. XGBoost creates models quickly because it is suitable for parallelization. It is used for classification and regression and , it is widely used (28).

Multilayer perception (MLP)
MLP is a neural network model with input, output and at least one hidden neuron layer. All of these layers are fully interconnected. It was developed by Rumelhart, Hinton, and Williams (4). MLP is a supervised learning algorithm. Input data coming to the input layer is processed and transmitted to the middle layer. The output of each layer becomes the input of the next layer. This process continues until the output layer. When the data is processed, it is multiplied by the weights in the connections. As a result of the operation, the error rate is calculated. The weights are optimized. The weights are recalculated to minimize the error rate (29).

RESULTS AND DISCUSSION

Objects close to the coated parts impair the accuracy of the model, so firstly the data concerned the coated parts should be extracted. Mask RCNN algorithm was trained to detect the concerned region on the image. The validation of the model was tracked computing its loss scores. The loss scores in Table 2 proves that the model was trained with high accuracy.

Table 2: The loss scores of train and validation dataset.

	Train	Validation
Loss	0.4250	0.4123
rpn_class_loss	0.0034	0.0038
rpn_bbox_loss	0.0509	0.0243
mrcnn_class_loss	0.0057	0.0061
mrcnn_bbox_loss	0.0405	0.0620
mrcnn_mask_loss	0.3245	0.3161

Figure 3a and b indicate the ground truth and predicted mask respectively. The intersection of over union (IoU) metric was used to determine the accuracy of the masked region on the coated plates. The IoU results are presented in Table 3. As seen in Table, the IoU scores vary between 0.92 and 0.97. These results prove that the reliability of the results is very high and Mask RCNN algorithm detects the region we concern on the plates accurately. Thereafter, the masked region was extracted from the image for the next step. The extracted data are presented in Figure 4.

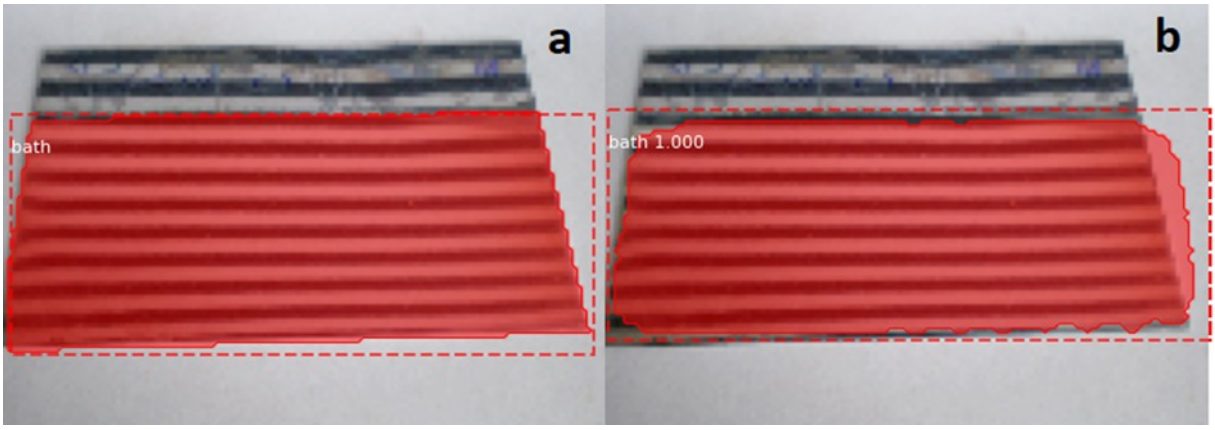

Figure 3: The ground truth (a) and predicted (b) panels as examples.

Table 3: The intersection over union (IoU) of validation dataset.

Validation Sample	Intersection Over Union (IoU)
1	0.94
2	0.97
3	0.92
4	0.93
5	0.97
6	0.94
7	0.97
8	0.93
9	0.97
10	0.97

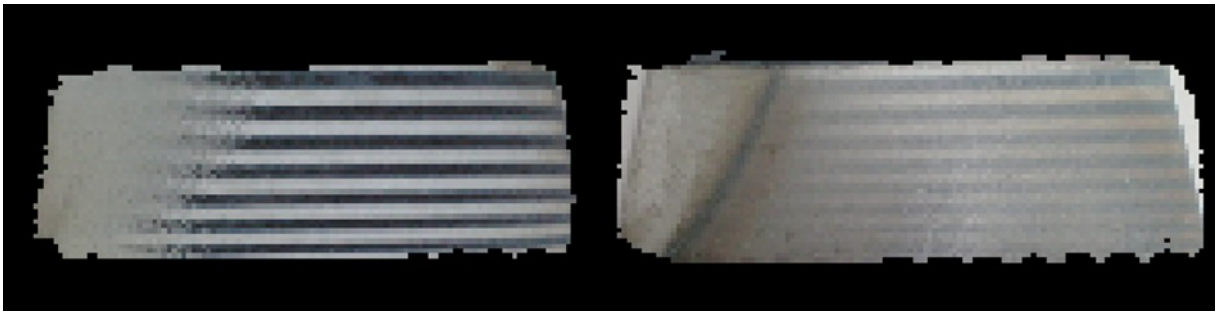

Figure 4: The acidic zinc coated plate samples extracted from the redundant data using Mask RCNN algorithm.

As seen in Figure 4, the algorithm has extracted the relevant region from the plate images with high accuracy. This proves that the unnecessary data can be removed from the industrially coated part images.

Figure 5 indicates the zinc coated panels. The black lines on the plates (Figure 5a) are not real, but a reflection. The number of pixels belonging to the black lines is related to the brightness of the surface. Actually, it is not possible to distinguish bright and smooth matte surfaces from the images. Therefore, to measure the brightness of the surface from the image, the apparatus in Figure 6 was set up and taken the pictures of the coated plates. The clearer the black lines, the brighter the coated surface. The regions where the black lines are interrupted indicate that the surface of the plate is matte (Figure 5b). The black lines on the plates, which indicates the brightness degree, are affected by the bath composition (coating conditions).

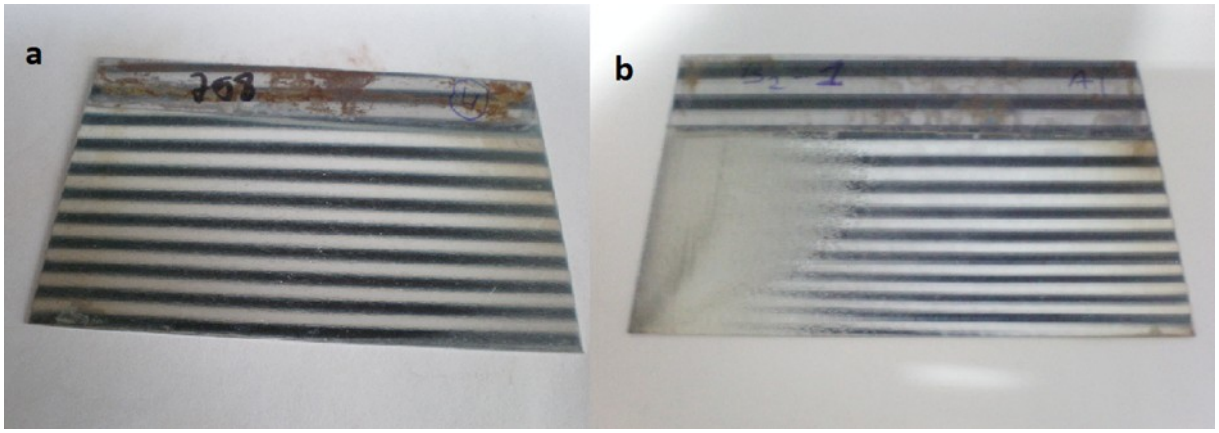

Figure 5: Two sample panels coated with acidic zinc.

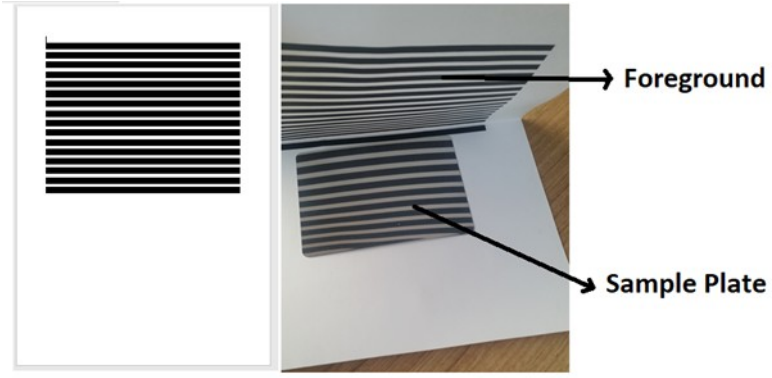

Figure 6: The apparatus of taking a picture.

The code and pictures used to count the black lines are presented in Figure 7. The interrupted black lines in Figure 7a depict the matte regions on the plate. When Figure 7a and b are compared, the matte and bright regions on the plates are compatible with one another. These results confirm that the technique used in this study is an effective tool to define the brightness degree of the plates. The appearance of the plates was also checked by naked eye. It was found that the order of outputs was compatible with the ones checked by naked eye.

```
img_gray_px=np.zeros([height,width,1], dtype=np.uint8)+255

height,width,_=img_r.shape

pix_num=0

for i in range(height):
  for j in range(width):
    if (img_gray[i,j] > 0 and img_gray[i,j] < 75):
      if (i> 50 and j>20) and (i < 220):
        img_gray_px[i,j]=img_gray[i,j]
      pix_num=pix_num+1

horizontalAppendedImg = np.hstack((img_gray_px.reshape(height,width),img_gray))
cv2_imshow(horizontalAppendedImg), print("pixel number:",pix_num)
```

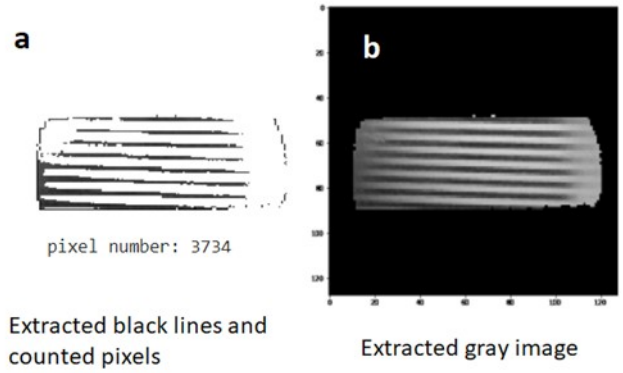

Figure 7: The code and pictures used to count the black lines.

The acidic zinc electroplating bath composition was trained in accordance with the brightness (the number of black line pixels). Four machine learning algorithms and one neural network were used to train the models. Threshold value was specified to binarize the outputs. The threshold value was chosen as 3500 pixels. The plates having the pixel number above this threshold was defined as 1 (Pass). The other panels were coded as 0 (Fail).

Accuracy, F1, precision, and recall scores were used to assess the validity of the models. Accuracy shows the ratio of accurately predicted values to the total dataset. This parameter alone is not sufficient to judge the whole model. Hence, F1 score, precision, and recall metrics were considered. Particularly, F1 score is a very significant metric to select the best model because it indicates the harmonic mean of recall and precision values. These metrics are computed via the confusion matrix. The confusion metrics of the models are demonstrated in Table 6. Accuracy, recall, precision and F1 scores were calculated using Eq. 1-4. The abbreviations of TP, TN, FP and FN are explained in Table 4.

$$Accuracy = (TP + TN) / (TP + FP + TN + FN) \quad \text{(Eq. 1)}$$

F1 score = 2*Precision*Recall / (Precision + Recall) (Eq. 2)

Precision = TP / (T0P + FP) (Eq. 3)

Recall = TP / (TP + FN) (Eq. 4)

Recall refers that what proportion of actual positives (TP) is estimated accurately. *Precision* depicts what proportion of estimated positives are actually 1. *F1 score* is the weighted average of recall and precision scores.

Table 4: The map of confusion matrix.

Confusion Matrix		**Y-predicted**	
		0	**1**
Y-true	**0**	True Negative (TN)	False Positive (FP)
	1	False Negative (FN)	True Positive (TP)

Table 5 displays the metric results of the models used. It was found that RF model is the best model to predict the quality of coated plates because its F1 score is higher than the others. The samples coded 0 are totally predicted accurately. Only two samples coded 1 are predicted wrong. The second-best model is MLP (F1 score 0.85). This model correctly predicted 64 out of 74 samples, but 9 samples were estimated wrong (Table 6). The other models have low accuracies. The success of models (F1 score was considered) was acquired in order of RF > MLP > SVC > GP > XGBoost (Table 5).

Table 5: The metrics of the ML and MLP algorithms for brightness.

ML Methods	**Accuracy**	**F1 score**	**Precision**	**Recall**
MLP	0.88	0.88	0.84	0.91
SVC	0.84	0.83	0.81	0.86
GP	0.68	0.65	0.67	0.63
XGBoost	0.59	0.69	0.54	0.94
RF	0.97	0.97	1	0.94

Table 6. The confusion matrix results of brightness.

MLP		**Y-predicted**	
		0	**1**
Y-true	**0**	33	6
	1	3	32

SVC		**Y-predicted**	
		0	**1**
Y-true	**0**	32	7
	1	5	30

GP		**Y-predicted**	
		0	**1**
Y-true	**0**	28	11
	1	13	22

XGBoost		**Y-predicted**	
		0	**1**
Y-true	**0**	11	28
	1	2	33

RF		**Y-predicted**	
		0	**1**
Y-true	**0**	39	0
	1	2	33

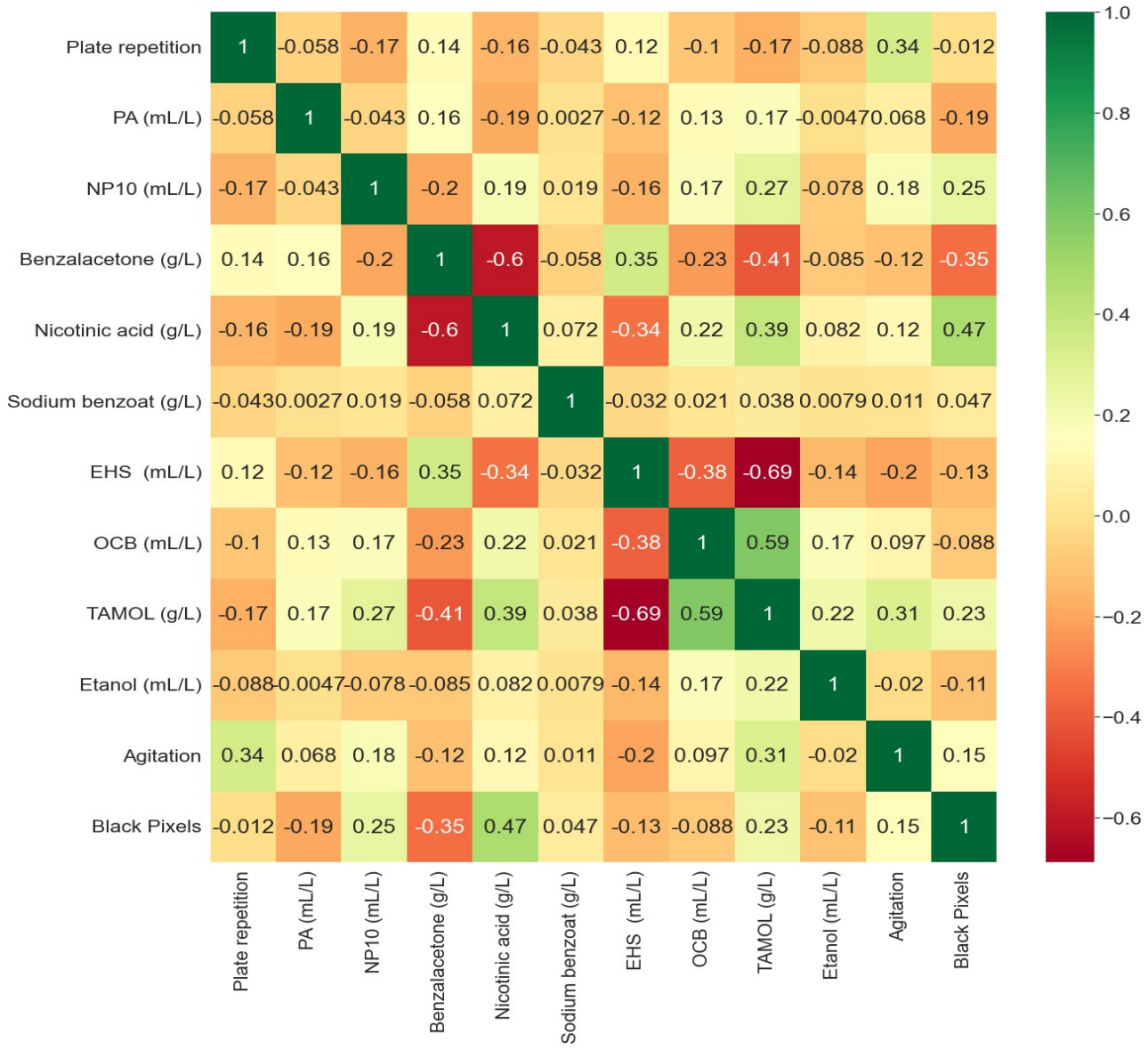

Figure 8: Heatmap of the feature weight matrix.

The heatmap was used to show the relationship between features (inputs) and brightness. Heatmap is a powerful tool to understand the relationship among the parameters at a glance with colors. As seen in Figure 8, the chemical increasing the brightness the most is nicotinic acid. A direct association between nicotinic acid and brightness is 0.47. Benzalacetone indicated the decreasing effect on the brightness (-0.35). Tamol and NP 10 chemicals also showed the brightness enhancing effect. The chemicals enhancing the brightness were acquired in order of nicotinic acid > NP10 > tamol > agitating > sodium benzoate. The other chemical showed the negative effect on the brightness.

Figure 9 indicates the importance of process parameters and organic chemicals in the electroplating. Random Forest algorithm was utilized to find the importance of the features (input parameters). Nicotinic acid has the most impact on the brightness of the coating. This result is compatible with the results acquired from the heatmap.

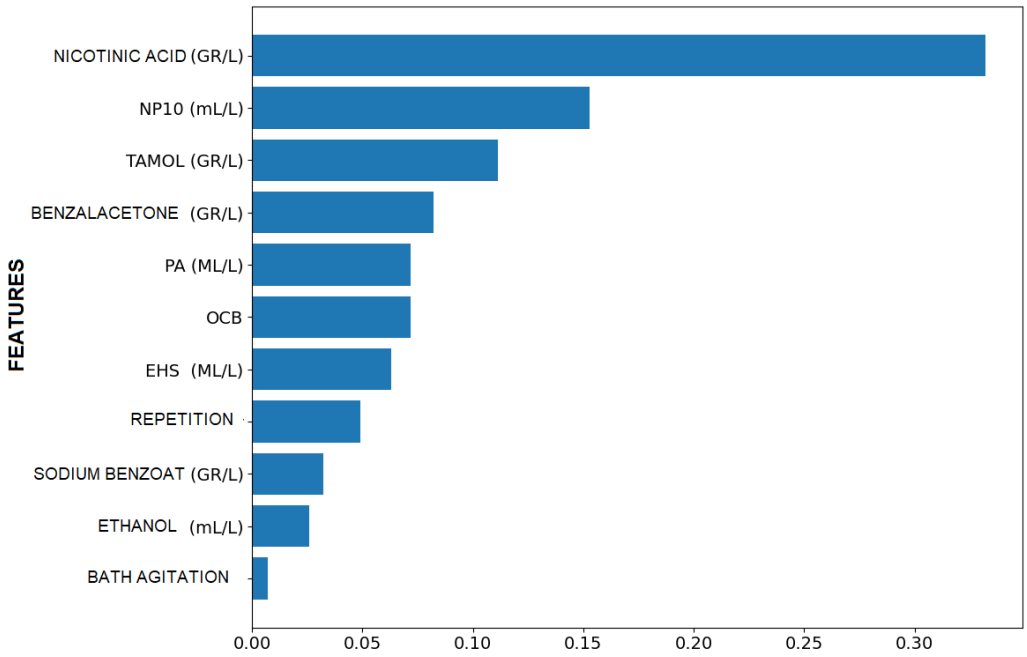

Figure 9: The importance of the chemicals in the electroplating bath.

As a result, this study proved that it is possible to measure the brightness of the coated parts using image processing technique. Even though this technique is an effective and strong technique, it has some problems to overcome. The blackness on the plates may sometimes be caused by a coating defect. As seen in Figure 9b, the coated plate is although almost completely matte, the red region on the plate (Figure 9a) is detected as bright by algorithm. In our study, since the error resulting from coating defects was seldom, the order of brightness and quality of plates did not change. It is possible to overcome this problem using different colors for the reflection lines on the plates. These colors may be fully blue, red or green. In this state, a colored image should be used to count the colored pixels. In our further studies, it is planned to use blue colored lines or circles to measure the brightness of the coating.

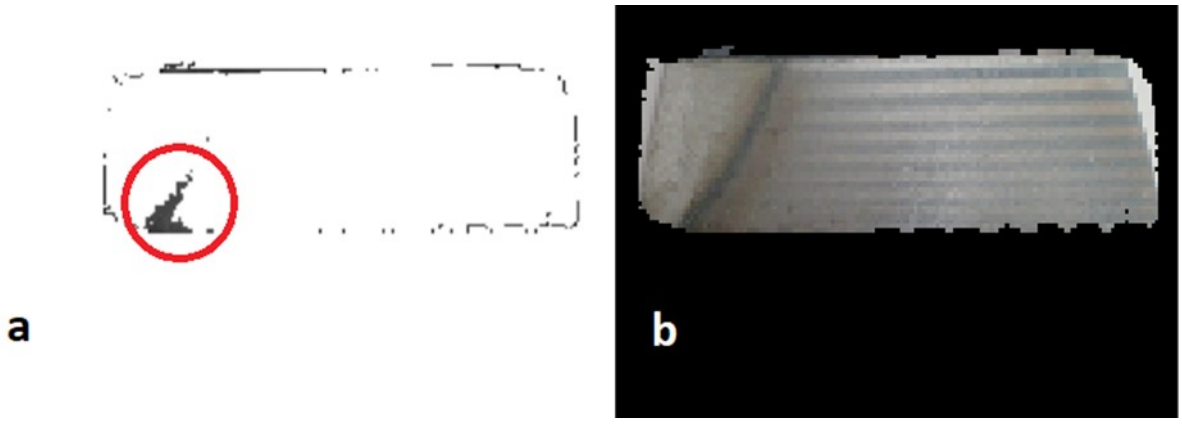

Figure 10: The image related to the brightness (left) and extracted panel.

CONCLUSION

In this study, Mask RCNN algorithm was used to extract the concerned data from the image. Image processing technique was used to count the pixels of the shape reflected from the foreground image. The number of pixels was taken as a measure of brightness. ML algorithms were used to classify the coated parts in accordance with their brightness. Four ML algorithms and one neural network were utilized to train the dataset. It was found that the RF model was the best model to predict the quality of the coating. Its accuracy, F1, precision and recall scores were found to be 0.97, 0.97, 1, 0.94 respectively.

The chemicals affecting the brightness in the zinc electroplating bath was investigated using heatmap method. The heatmap indicated that nicotinic acid has the most positive impact increasing the brightness of the coating.

This study revealed three important results;

✓ Mask RCNN can be used to remove the redundant data from the image.
✓ Image processing technique can be used to measure the brightness of the coating.
✓ ML algorithms can be used to predict the quality of the coating performed in the zinc electroplatings bath in accordance with their brightness.

In a nutshell, to measure the brightness of the coated parts, a technical set up should be used. In this set up, a suitable reflecting foreground should be chosen. This foreground should contain some colored shapes which will be reflected on the coated parts. The pixels of this shape correspond to the brightness of the coated parts. In the industry, a similar set-up can be used to classify the coated parts as “Fail” and “Pass” on the production line. The object near the coated parts weakens the prediction power of the model. Therefore, the redundant object should be extracted using Mask RCNN algorithm. Image processing technique can be implemented to the extracted data to count the pixels reflected from the foreground. Foreground color and shape is crucial to count the pixels. If the color and shape of the foreground are similar to the defect results from the coating error, the results may be inaccurate. To avoid this problem the different color and shape should be used for the reflection. In our further studies, blue or red colored lines or circles will be utilized to prevent the interference resulting from the coating defect.

CONFLICT OF INTEREST

The authors declare that they have no known competing financial interests or personal relationships that could have appeared to influence the work reported in this paper.

ACKNOWLEDGMENTS

The experiments reported in this paper were fully performed at TUBITAK ULAKBIM, High Performance and Grid Computing Center (TRUBA resources).

REFERENCES

1. Safavi MS, Walsh FC. Electrodeposited Co-P alloy and composite coatings: A review of progress towards replacement of conventional hard chromium deposits. Surface and Coatings Technology. 2021 Sep;422:127564. Available from: <URL>,

2. Fotovvati B, Namdari N, Dehghanghadikolaei A. On Coating Techniques for Surface Protection: A Review. JMMP. 2019 Mar;3(1):28. Available from: <URL>.

3. Gu Y, Liu J, Qu S, Deng Y, Han X, Hu W, et al. Electrodeposition of alloys and compounds from high-temperature molten salts. Journal of Alloys and Compounds. 2017 Jan;690:228–38. Available from: <URL>.

4. Gérard B. Application of thermal spraying in the automobile industry. Surface and Coatings Technology. 2006 Oct;201(5):2028–31. Available from: <URL>.

5. Bobzin K, Brögelmann T, Kalscheuer C, Liang T. High-rate deposition of thick (Cr,Al)ON coatings by high speed physical vapor deposition. Surface and Coatings Technology. 2017 Aug;322:152–62. Available from: <URL>.

6. Xia F, Xu H, Liu C, Wang J, Ding J, Ma C. Microstructures of Ni–AlN composite coatings prepared by pulse electrodeposition technology. Applied Surface Science. 2013 Apr;271:7–11. Available from: <URL>.

7. Safavi MS, Etminanfar M. A review on the prevalent fabrication methods, microstructural, mechanical properties, and corrosion resistance of nanostructured hydroxyapatite containing bilayer and multilayer coatings used in biomedical applications. J Ultrafine Grained Nanostruct Mater [Internet]. 2019 Jun [cited 2022 Oct 17];52(1). Available from: <URL>.

8. Katırcı R, Yılmaz EK, Kaynar O, Zontul M. Automated evaluation of Cr-III coated parts using Mask RCNN and ML methods. Surface and Coatings Technology. 2021 Sep;422:127571. Available from: <URL>.

9. Bayati MR, Shariat MH, Janghorban K. Design of chemical composition and optimum working conditions for trivalent black chromium electroplating bath used for solar thermal collectors. Renewable Energy. 2005 Nov;30(14):2163–78. Available from: <URL>.

10. Kul M, Oskay K, Erden F, Akça E, Katirci R, Köksal E, et al. Effect of Process Parameters on the Electrodeposition of Zinc on 1010 Steel: Central Composite Design Optimization. Int J Electrochem Sci. 2020 Oct;9779–95. Available from: <URL>.

11. Mirkova L, Maurin G, Krastev I, Tsvetkova C. Hydrogen evolution and permeation into steel during zinc electroplating; effect of organic additives. Journal of Applied Electrochemistry. 2001;31(6):647–54. Available from: <URL>.

12. Arnold JO. The Metallurgy of Steel. Nature. 1912 May;89(2222):315–6. Available from: <URL>.

13. Yang D, Wang X, Zhang H, Yin Z yu, Su D, Xu J. A Mask R-CNN based particle identification for quantitative shape evaluation of granular materials. Powder Technology. 2021 Nov;392:296–305. Available from: <URL>.

14. Kiliçarslan S, Celik M. KAF + RSigELU: A nonlinear and kernel-based activation function for deep neural networks. Neural Comput & Applic. 2022 Aug;34(16):13909–23. Available from: <URL>.

15. Kiliçarslan S, Celik M. RSigELU: A nonlinear activation function for deep neural networks.

Expert Systems with Applications. 2021 Jul;174:114805. Available from: <URL>.

16. Adem K, Kilicarslan S. COVID-19 Diagnosis Prediction in Emergency Care Patients using Convolutional Neural Network. Akufemubid. 2021;21(2):300–9. Available from: <URL>.

17. Adem K. Impact of activation functions and number of layers on detection of exudates using circular Hough transform and convolutional neural networks. Expert Systems with Applications. 2022 Oct;203:117583. Available from: <URL>.

18. Simonyan K, Zisserman A. Very Deep Convolutional Networks for Large-Scale Image Recognition. 2014 [cited 2022 Oct 17]; Available from: <URL>.

19. He K, Zhang X, Ren S, Sun J. Deep Residual Learning for Image Recognition. In: 2016 IEEE Conference on Computer Vision and Pattern Recognition (CVPR) [Internet]. Las Vegas, NV, USA: IEEE; 2016 [cited 2022 Oct 17]. p. 770–8. Available from: <URL>.

20. Szegedy C, Vanhoucke V, Ioffe S, Shlens J, Wojna Z. Rethinking the Inception Architecture for Computer Vision. In: 2016 IEEE Conference on Computer Vision and Pattern Recognition (CVPR) [Internet]. Las Vegas, NV, USA: IEEE; 2016 [cited 2022 Oct 17]. p. 2818–26. Available from: <URL>

21. Chollet F. Xception: Deep Learning with Depthwise Separable Convolutions. In: 2017 IEEE Conference on Computer Vision and Pattern Recognition (CVPR) [Internet]. Honolulu, HI: IEEE; 2017 [cited 2022 Oct 17]. p. 1800–7. Available from: <URL>.

22. Yu Y, Zhang K, Yang L, Zhang D. Fruit detection for strawberry harvesting robot in non-structural environment based on Mask-RCNN. Computers and Electronics in Agriculture. 2019 Aug;163:104846. Available from: <URL>.

23. Kumar G, Bhatia PK. A Detailed Review of Feature Extraction in Image Processing Systems. In: 2014 Fourth International Conference on Advanced Computing & Communication Technologies [Internet]. Rohtak, India: IEEE; 2014 [cited 2022 Oct 17]. p. 5–12. Available from: <URL>.

24. Hull R. Current Density Range Characteristics, Their Determination and Application. Proc Am Electroplaters Soc. 1939;27:52.

25. Hu J, Sun Y, Li G, Jiang G, Tao B. Probability analysis for grasp planning facing the field of medical robotics. Measurement. 2019 Jul;141:227–34. Available from: <URL>.

26. Reza M, Miri S, Javidan R. A Hybrid Data Mining Approach for Intrusion Detection on Imbalanced NSL-KDD Dataset. ijacsa [Internet]. 2016 [cited 2022 Oct 17];7(6). Available from: <URL>.

27. Vapnik VN. The Nature of Statistical Learning Theory [Internet]. New York, NY: Springer New York; 2000 [cited 2022 Oct 17]. Available from: <URL>.

28. Chen T, Guestrin C. XGBoost: A Scalable Tree Boosting System. In: Proceedings of the 22nd ACM SIGKDD International Conference on Knowledge Discovery and Data Mining [Internet]. San Francisco California USA: ACM; 2016 [cited 2022 Oct 17]. p. 785–94. Available from: <URL>.

29. Rumelhart DE, Hinton GE, Williams RJ. Learning Internal Representations by Error Propagation. In: Readings in Cognitive Science [Internet]. Elsevier; 1988 [cited 2022 Oct 17]. p. 399–421. Available from: <URL>.